Invasive Sea Lamprey Detection and Characterization Using Interdigitated Electrode (IDE) Contact Sensor

Ian González-Afanador, *Member, IEEE*, Hongyang Shi, *Member, IEEE*, Christopher Holbrook, Xiaobo Tan, *Fellow, IEEE*, and Nelson Sepúlveda, *Senior Member, IEEE*

***Abstract*—The ability to monitor invasive sea lamprey (Petromyzon marinus) populations in the Laurentian Great Lakes is critical to protecting the region's $7 billion USD fishing industry and preserving its biodiversity. Monitoring these invaders requires considerable fieldwork and human power, making remote lamprey detection systems attractive for their continuous monitoring capabilities and potential for workload reduction. However, a lack of available methods for detecting sea lamprey hampers development of such systems. Here we present a sensor composed of two exposed planar interdigitated electrodes (IDE) along with a DC measurement system for the detection of lamprey attachment underwater. Measuring voltage instead of impedance, reduces cost and signal processing complexity, making the device more attractive for field deployment. The system is calibrated to a baseline output voltage and deviations from this baseline occur when objects touch the IDE. Validation was done through testing on live adult sea lampreys using video recordings to correlate lamprey attachments to the sensor response. Three response types were identified corresponding to different attachments: sustained, short and sliding-sustained. Sensor response to sustained and sliding-sustained attachments showed a characteristic exponential decay whereas the response due to short attachments was indistinguishable from measurement noise. Lamprey size was found to have a weak linear correlation with both response parameters, positive for the voltage drop and negative for the time constant of voltage drop. A representative circuit for the lamprey-sensor interaction is proposed and simulated using element values calculated from the response parameters. The response of the model shows agreement with experimental data.**

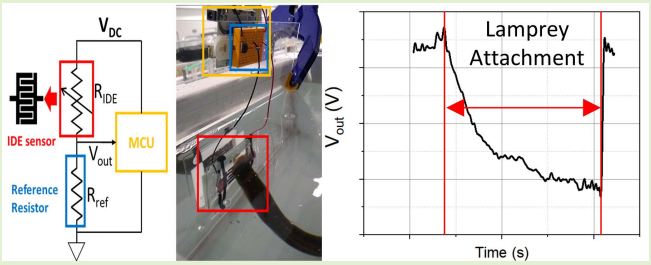

***Index Terms*—Interdigitated electrode sensors, wildlife detection, correlation analysis, underwater biological contact sensing, invasive species control.**

Manuscript received August 11, 2021; revised September 22, 2021; accepted October 12, 2021. Date of publication October 26, 2021; date of current version December 14, 2021. This work was supported in part by the Great Lakes Fishery Commission under Grant 2018_TAN_54069, in part by the Michigan State University (MSU) Strategic Partnership Grant 16-SPG-Full-3236, and in part by the NSF through the Graduate Research Fellowship Program (GRFP) under Grant DGE-1848739. The associate editor coordinating the review of this article and approving it for publication was Dr. Yong Zhu. *(Corresponding author: Ian González-Afanador.)*

This work involved human subjects or animals in its research. Approval of all ethical and experimental procedures and protocols was granted by Michigan State University and the Institutional Animal Care and Use Committee (IACUC), under Approval No. AAALAC Unit 1047, and performed in line with the following regulations and requirements: USDA regulations (9 CFR Parts 1, 2, and 3), the Public Health Service Policy on Humane Care and Use of Laboratory Animals (PHS Policy), the Guide for the Care and Use of Laboratory Animals, 8th Edition (the Guide), and the Guide for the Care and Use of Agricultural Animals in Research and Teaching, 3rd Edition (Ag Guide).

Ian González-Afanador, Hongyang Shi, Xiaobo Tan, and Nelson Sepúlveda are with the Electrical and Computer Engineering Department, Michigan State University, East Lansing, MI 48824 USA (e-mail: gonza834@msu.edu; shihong1@egr.msu.edu; xbtan@egr.msu.edu; sepulve6@msu.edu).

Christopher Holbrook is with the U.S. Geological Survey, Great Lakes Science Center, Hammond Bay Biological Station, Millersburg, MI 49759 USA (e-mail: cholbrook@usgs.gov).

This article has supplementary downloadable material available at https://doi.org/10.1109/JSEN.2021.3122884, provided by the authors.

Digital Object Identifier 10.1109/JSEN.2021.3122884

I. Introduction

NATIVE to the Atlantic Ocean, sea lampreys (*Petromyzon marinus*) are an invasive fish species in the Laurentian Great Lakes region. As parasitic organisms, they feed by attaching to other fish using their suction cup-like mouth and scraping a hole through the skin to suck on the prey fish's blood and other bodily fluids [1]. While it is debated whether sea lampreys are native to Lake Ontario, they have been reported in the lake since at least 1888 [2]. It is believed they spread from Lake Ontario to Lake Erie, and later to the rest of the Great Lakes, through the Welland Canal which began operation in 1829. The presence of sea lampreys in Lake Erie was first confirmed in 1921 [3], and by 1938 they had spread to the remaining Great Lakes [4]. They quickly exploded in number and contributed to a decline in large fish stocks causing a devastating decrease in commercial fishing yields, which resulted in the effective collapse of this industry in many parts of the region [5]. Lake trout (Salvelinus namaycush), lake whitefish (Coregonus clupeaformis), and burbot (Lota lota), which were lampreys' preferred prey, were depleted or extirpated from much of the Great Lakes [6].As these were the main predators in the region, their disappearance opened

1558-1748 © 2021 IEEE. Personal use is permitted, but republication/redistribution requires IEEE permission.
See https://www.ieee.org/publications/rights/index.html for more information.

Authorized licensed use limited to: Michigan State University. Downloaded on February 28,2022 at 16:02:46 UTC from IEEE Xplore. Restrictions apply.

the door for other invasive species such as rainbow smelt (Osmerus mordax) and alewife (Alosa pseudoharengus) which created intense competition for species not directly threatened by sea lampreys [7], further destabilizing the ecological balance of the region. While their numbers have been brought under control through the use of lamprey selective pesticides and other control measures implemented by the Sea Lamprey Control Program (SLCP) [8], monitoring sea lamprey populations is still critical to avoiding catastrophic population growth, which would threaten a fishing industry employing around 75,000 people and valued at $7 billion USD annually [9].

Current monitoring approaches rely extensively on fieldwork, requiring capturing lampreys in each lake's tributary system to perform mark-recapture studies and get local population estimates, which are then combined to obtain a population estimate for the entire lake [10], [11]. One drawback of this approach is the significant effort and equipment needed to execute it. Traps must first be placed in strategic, often remote, locations to capture sea lampreys and must then be checked daily, requiring considerable human power and resources be dedicated to this task. Recently, the use of environmental DNA (eDNA), a molecular surveillance technique that uses polymerase chain reaction (PCR) to look for species- specific genetic signatures in water samples taken from the areas of interest, has been tested in the field with some success and suggested as a possible alternative to trap-based monitoring [12]. However, this approach remains sensitive to flow rates in the collection area and has yet to be widely adopted. Remote lamprey sensing systems present another alternative surveillance technique; these systems could factor in environmental disturbances in their measurements, enhancing operational capabilities by allowing for continuous population monitoring. Moreover, by exploiting the behavior of the species during the design of these systems, it results in a less disruptive assessment technique than tagging as well as reduces dependence on traps. In addition to workload reduction for conservation agencies like the SLCP, trap-free detection could provide greater insights into the behavior of these fish at times and locations where capture or direct observation has been historically limited. However, the lack of commercially available sensors which can detect lampreys and the necessary scale of deployment for these systems to be effective are major hurdles in the development of such systems. There have been efforts to develop capacitive pressure sensing arrays capable of detecting positive and negative pressures [13], which could detect sea lamprey by taking advantage of their tendency to use their oral disks to attach to objects underwater. Laboratory testing of these sensors using a polymer suction cup produced promising results; however, the quickly changing pressure exerted by the lamprey proved difficult to capture with the implemented measurement system [14]. Additionally, capacitive interference due to the dielectric nature of biological material may have also contributed to difficulties with these measurements.

The development of the sensing system presented in this study took inspiration from the interdigitated electrode (IDE) electrode structure, which is widely employed in electrochemical sensors. The working principle behind these devices uses the change in impedance seen across the electrodes, caused by the surface accumulation of the compounds, as the sensing signal [17]. These sensors have been widely utilized as chemical detectors [18] and biosensors [19]–[21] and they use electrochemical impedance spectroscopy (EIS) analysis to perform label-free detection and concentration measurements. As the surface accumulation that drives the sensing signal could be described as the aggregate of multitudes of incredibly small discrete "contact" events [21], it is possible this sensing principle could be adapted on a larger scale for the task of underwater biological contact sensing. This work presents a novel use of the IDE structure as an underwater contact sensor for invasive sea lamprey detection.

The sensors are composed of two separate planar electrodes with interlocking fingers in close proximity, but electrically isolated when in air. They are encapsulated in a way that only the sensing electrode area is exposed to water (see Fig. 1-A). The sensing mechanism applies a direct current (DC) bias to a voltage divider formed by a reference resistor and the IDE sensor, monitors the voltage across the electrodes and relates its abrupt changes to electrode impedance caused by attachment/detachment of the lamprey, effectively working as a type of electric switch/indicator. This approach was selected over more sophisticated impedance measurement schemes, which require additional components and signal processing, that would increase the cost and complexity of the device making it less suitable for the large-scale deployments necessary for the system to be effective at monitoring sea lamprey populations. While electrochemical IDE sensors use an alternating current (AC) probing signal to directly determine the impedance/capacitance (or its frequency response) during EIS [22], the approach taken here is akin to an indirect impedance measurement; since the probing signal is DC, the steady state value of the response is assumed to be due to the effective resistance between the electrodes with any capacitive behavior being captured in the transient response of the sensor. When the sensor is submerged in water, an electrical connection is formed between both electrodes resulting in a measurable baseline, which can be disturbed during interaction with a foreign object, e.g., lamprey contact. This mechanism introduces a degree of selectivity in the contact sensing, as the system will react differently to contact sources with different conductivities, relative to the conductivity of the surrounding medium —in this case, lake water. This behavior opens the door to characterization of the contact source which is important as the American brook lamprey (Lampetra appendix) [23], northern brook lamprey (Ichthyomyzon fossor) [24], chestnut lamprey (Ichthyomyzon castaneus) [25] and the silver lamprey (Ichthyomyzon unicuspis) [26] are all native to the region and share behavioral patterns with sea lamprey that may lead to their interaction with these sensors.

Electrochemical IDE sensors enforce selectivity by functionalizing the electrode surface to have an affinity for bonding with the target molecule [27]. In the case of the device presented here, selectivity is partially enforced simply by the detection mechanism, as non-lamprey species are not likely to interact with the sensor for sustained time. During the adult life stage targeted by this work, the major distinction

Authorized licensed use limited to: Michigan State University. Downloaded on February 28,2022 at 16:02:46 UTC from IEEE Xplore. Restrictions apply.

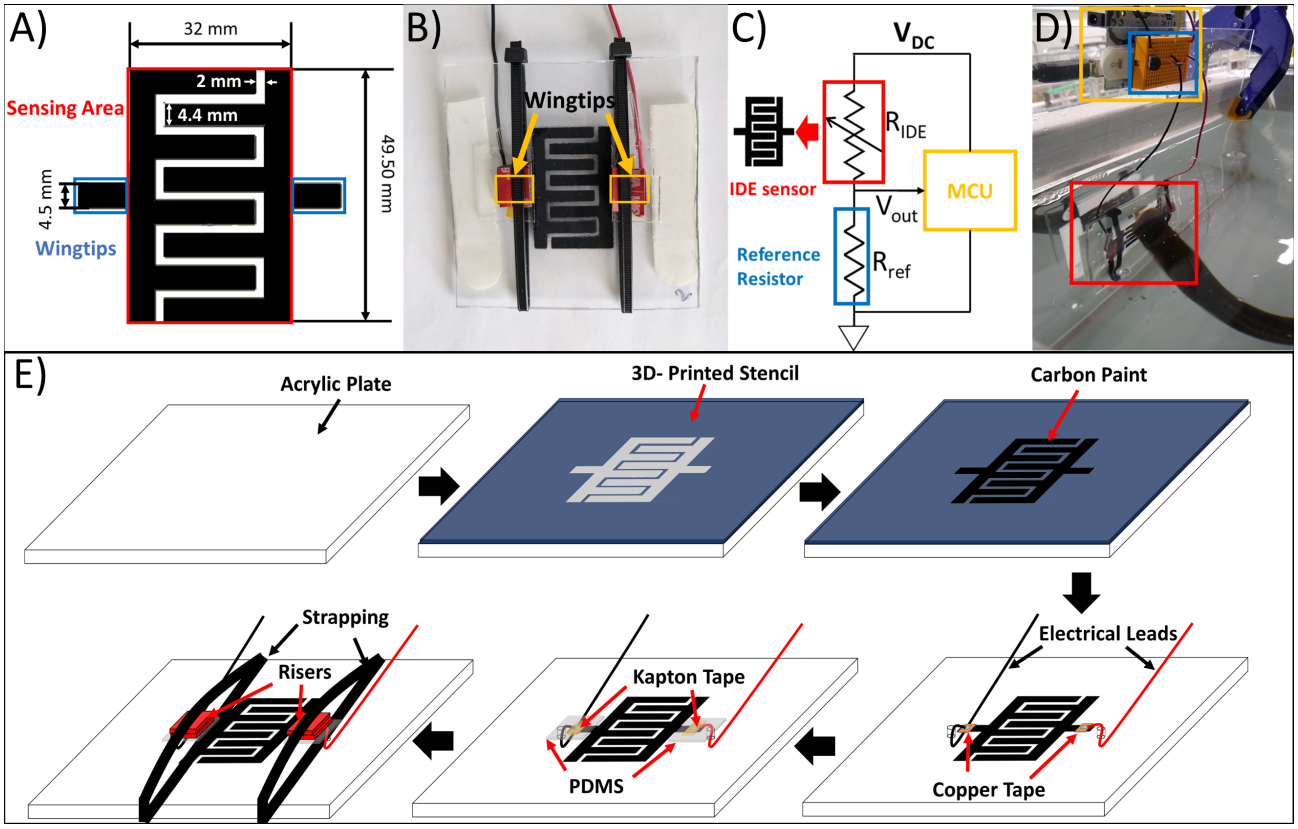

Fig. 1. (a) Schematic of IDE sensor geometry and dimensions; (b) Final manufactured device; (c) Measurement system schematic; (d) Implemented measurement system attached to an acrylic panel; (e) Device manufacturing process flow.

between native and invasive species of lamprey is their size, with adult sea lamprey typically being twice as large (35 – 60 cm) as the native species (10.3 – 32.6 cm) [28]. Therefore, the sensor response must be analyzed to determine if there is a correlation between the size of the lamprey and the response parameters.

This paper covers the design and manufacturing process for an underwater IDE contact sensor for sea lamprey attachment detection, including an overview of the testing methodologies used to validate the device through experiments with live sea lampreys. Data from the experiments were analyzed to characterize the disturbance caused by lamprey attachment on the sensor and observe whether it was distinguishable from measurement noise. The experimental results are presented along with a correlation study between the identified response parameters and lamprey size parameters with the goal of enhancing the utility of the sensor by exploring the characterization of lamprey size from the sensor response. Finally, a simple representative circuit modeling the lamprey-sensor interaction is proposed and simulated using component values extracted from the sensor response data.

II. Approach

A. Device Design and Fabrication

Clear acrylic panels were used as the substrate for the IDE sensor to allow visual monitoring of lamprey attachment events and correlate these to the electrical measurements of the system. The specified operating conditions of the sensor preclude utilizing any conductive materials that are prone to corrosion, as this would not only hamper its functionality but also lead to unintended contamination of the freshwater systems where it is to be deployed. Marine-grade conductive carbon spray paint (838AR - Total Ground Carbon Conductive Coating by MG Chemicals) was selected as the electrode material for our protypes due to its low cost, relatively high conductivity and ease of application. The electrodes were patterned onto the acrylic substrates using 0.6 mm thick 3D-printed stencils developed in AutoDesk's Solidworks 3D modeling suite. This fabrication process allowed for an iterative approach at the device design stage, where we tested different geometries, overall size, electrode finger length and width, and distance between the electrical lead attachments and noted the effect on the magnitude of sensor response to contact from a conductive probe and a human hand. Multiple prototype generations were tested until reaching the final design which showed the best response magnitude under test conditions.

A schematic of the final proposed device is shown in Fig. 1-A. The design consists of a small rectangular interdigitated electrode (sensing area of 32 mm × 49.50 mm) with wingtips to allow for attachment of electrical leads away from the sensing area. During preliminary experiments, it was observed that the sensitivity of the sensor increased with decreasing distance between the electrical leads (see Fig. 1-E); and the sensor design/configuration used (Fig. 1-A) allowed for the smallest possible distance that will still allow enough sensing area to include the lamprey's oral disk. Wingtips were added to the design to facilitate protection of the sensor-lead connection without having to sacrifice sensing area. It was

Authorized licensed use limited to: Michigan State University. Downloaded on February 28,2022 at 16:02:46 UTC from IEEE Xplore. Restrictions apply.

TABLE I
SEA LAMPREY SIZE PARAMETER MEASUREMENTS

Tag	Weight (g)	Length (cm)	Mouth Diameter (mm)
blue-018	255	44	44.8
blue-009	246	50	40.6
orange-002	176	42	40.4
orange-017	241	48	39.6
white-041	200	45	39.6
orange-025	161	39	38.0
white-028	117	38	37.9
blue-002	158	39	37.9
orange-004	177	40	37.8
orange-040	177	42	37.2
pink-034	144	39	36.9
pink-027	174	45	36.5
white-043	118	39	36.0
pink-035	143	40	34.7
orange-026	132	40	34.3
white-037	141	40	34.2
pink-029	124	38	33.9
blue-024	143	40	33.3
pink-028	128	40	33.0
orange-035	87	35	29.3

found that a gap of 2 mm between electrodes would facilitate stencil fabrication and any post-processing of the deposited traces, while also providing a detectable change in resistance upon lamprey's attachment. Trace width was selected to optimize the fill factor of the device under the area and separation constraints. Fig. 1-B shows the final manufactured device used for testing, and Fig. 1-E shows the device fabrication process beginning with a square acrylic panel substrate (approximately 102 mm × 102 mm), on which the 3D-printed stencil was attached using repositionable craft adhesive. A coat of conductive carbon paint was then deposited, allowed to cure for at least one hour, followed by a second coat which was cured for at least 12 hours. By following the manufacturer's instructions each coat should be approximately 25 μm thick, giving the device a total thickness of approximately 50 μm. After the paint was completely cured, the stencils were separated from the acrylic and any excess paint between the traces was removed using a cotton swab applicator with small amounts of isopropyl alcohol. Holes were then drilled just outside of the wingtips, which served as feedthrough vias for the electrical leads. A small piece of copper tape was soldered onto the leads and used to create a conductive contact between the carbon trace and the leads. This connection was then secured, first by fixing it to the acrylic plate using Kapton tape, followed by an encapsulation using polydimethylsiloxane (PDMS) for waterproofing, finishing with strapping and use of high-strength tape for a robust attachment to the acrylic plate. To fix the position of the leads on the backside of the plate, small amounts of hot glue were utilized. Finally, two velcro tabs were attached to the back of the acrylic panel, so that it could be attached to a larger panel housing the measurement system for testing.

After the devices were manufactured, the sensor response to open and short-circuit tests was confirmed in air using a handheld multimeter. For the open-circuit test, an infinite resistance across the two separate IDEs was measured. For the short circuit test, both electrodes were connected using a piece of copper tape; and the test confirmed a very low resistance (∼100 Ohms) between both copper tape leads. After validating the device's operation ex-situ, their integration in a system for underwater deployment and testing followed.

B. Measurement System

In order to measure the sensor response, a DC voltage divider circuit was used, which converted the change in impedance across the electrodes to a change in voltage. This measurement approach is viable because the precision requirements for simple contact detection are lower than those for electrochemical characterization and detection. We utilized an Arduino microcontroller platform (MCU block in Fig. 1-C) to provide the 5 V DC bias (V_{DC}) to the voltage divider circuit and measured the output voltage at a 10 Hz sampling frequency using its integrated analog-to-digital converter (ADC) module. The schematic for the system is shown in Fig. 1-C. This configuration also allows for the calibration of the measurement system in the presence of water through the reference resistor (R_{ref}). To this end, the device is submerged in water and the reference resistor is adjusted until the output voltage of circuit is approximately half of the DC bias, in this case ∼2.50 V. This results in an approximate value of the baseline resistance between the electrodes (R_{IDE}) due to water and enables a relationship between the output voltage and the change in resistance. Using a voltage divider analysis for the circuit shown in Fig. 2-A, the output voltage (V_{out}) can be calculated as:

$$V_{out} = V_{DC} * \left(\frac{R_{ref}}{R_{IDE} + R_{ref}} \right). \quad (1)$$

This equation only holds at all time instances if the circuit is purely resistive, and since water and animal flesh are dielectric materials, it is reasonable to expect some capacitive behavior from the IDE sensor. However, since the probing signal is DC, the capacitance will come into play only in the transient behavior of the response, meaning that (1) will still be a valid description of the steady state of the signal measured by the MCU unit. It should be noted that R_{ref} has a fixed resistance value, whereas R_{IDE} has a variable resistance that depends on any contact between the two isolated electrodes. In the performed experiments, the background R_{IDE} value (i.e., resistance before lamprey's contact) represents the water resistance between the electrodes (R_{water}). By selecting $R_{ref} = R_{water}$ and expressing $R_{IDE} = R_{water} \pm \Delta R$ (where ΔR represents the magnitude of the change in resistance across the electrodes and its sign indicates whether R_{IDE} is increasing or

Authorized licensed use limited to: Michigan State University. Downloaded on February 28,2022 at 16:02:46 UTC from IEEE Xplore. Restrictions apply.

decreasing) we can re-write (1) as:

$$V_{out} = V_{DC} * \left(\frac{1}{2 \pm \frac{\Delta R}{R_{water}}} \right). \quad (2)$$

It should be noted that the addition or subtraction of the $\Delta R/R_{water}$ term occurs when R_{IDE} increases or decreases, respectively. Thus, an increase in the resistance across the electrodes ($+\Delta R$) will correspond to a drop in the measured output voltage (V_{out}); and, correspondingly, a decrease in R_{IDE} ($-\Delta R$) will result in an increase in V_{out}. This allows for the distinction between two general types of contact: 1) when ΔR is negative, meaning R_{IDE} is lower than the surrounding medium (i.e., $R_{IDE} < R_{water}$), and 2) when ΔR is positive corresponding to an R_{IDE} which is higher than the medium (i.e., RIDE $> R_{water}$). Further characterization within those two categories is possible by examining the magnitude of the change in ΔR.

Fig. 1-D shows how the system was implemented for testing. The microcontroller platform and a small circuit protoboard housing the reference resistors were attached to the top of a larger acrylic panel measuring 304.8 mm × 304.8 mm using velcro tabs for easy replacement/modification if necessary. The sensor was then attached at the bottom of the acrylic panel, in order to allow for submerging the system without exposing the rest of the system to moisture – i.e., waterproofing.

C. Test Procedures

Experiments were performed at U.S. Geological Survey, Great Lakes Science Center's Hammond Bay Biological Station (HBBS) in Millersburg, MI. HBBS staff provided 20 male sea lamprey specimens, each tagged with a unique identifier for tracking purposes between experiments. The length, weight and mouth diameter of the lamprey were measured and recorded as they were tagged (see Table I).

As explained later in Section IV, the physical characteristics of the lampreys shown in this table were used to determine strength of correlation between the sensor response and each lamprey size parameter. Such correlation is of particular interest, because it would enhance the monitoring capabilities of the developed system from simple detection, to characterization of an attached lamprey's size, which may allow distinction between species or life stages.

Experiments were conducted in a 200 L rectangular aquarium tank (Fig. 2-A) supplied with aerated water from Lake Huron. The sensing panel was submerged in the tank and fastened using clamps before tests started. The sensor was calibrated to an output voltage of approximately 2.5 V, and a baseline measurement was recorded for several minutes before testing to ensure this baseline did not drift significantly due to water turbulence. The test procedure consisted of placing a lamprey into the tank and coaxing it (manually) into attaching to the sensor (see video S1 in Section 1 of the supplementary material). A closeup of how the sea lamprey's mouth looks while attaching to the sensor during testing can be seen in Fig. 2-B; as the image was taken from the opposite side of the sensor, through the tank wall, the lamprey

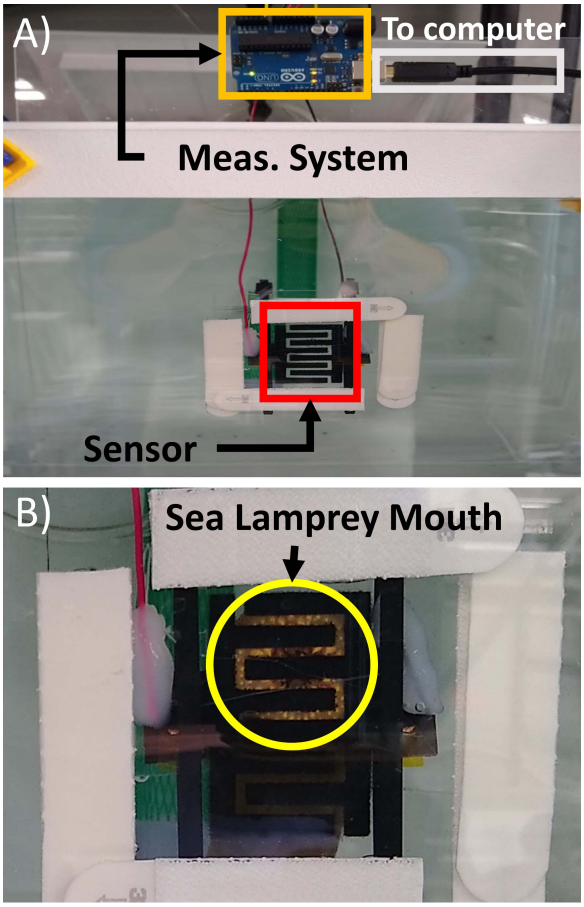

Fig. 2. (a) Sea lamprey holding tanks with sensing panel installed; (b) Lamprey attaching onto sensor during testing; view of the lamprey is obstructed by sensor traces as image was taken from the outside of the testing tank.

is partially obstructed by the electrodes. Video and voltage measurements were recorded until the lamprey detached from the sensor. An audio cue was triggered in the video in order to synchronize the recording and the data offline. On the first day of testing, 20 experiments were completed on the sensor, one with each lamprey of the cohort, with additional baseline measurements taken after halfway through testing. The baseline measurements were taken again, after all tests were completed for validation purposes. On the second day, 10 additional tests were completed with the lamprey cohort for validation purposes. Voltage data were then processed in OriginLab using a lowpass filter with a cut-off frequency of 0.25 Hz to filter out high frequency measurement noise associated with ADC readings such as input- referred noise and voltage regulation noise. Finally, a time offset was applied to the data in order to synchronize voltage measurements and video recording. Voltage data and video recordings from these tests were then cross-referenced to determine which disturbances in the baseline were caused by lamprey attachment events (see videos in Section 1 of the supplementary material).

III. Results

A. Sensor Response

Three distinct types of responses were identified from the sensor, each corresponding to a different type of attachment.

Authorized licensed use limited to: Michigan State University. Downloaded on February 28,2022 at 16:02:46 UTC from IEEE Xplore. Restrictions apply.

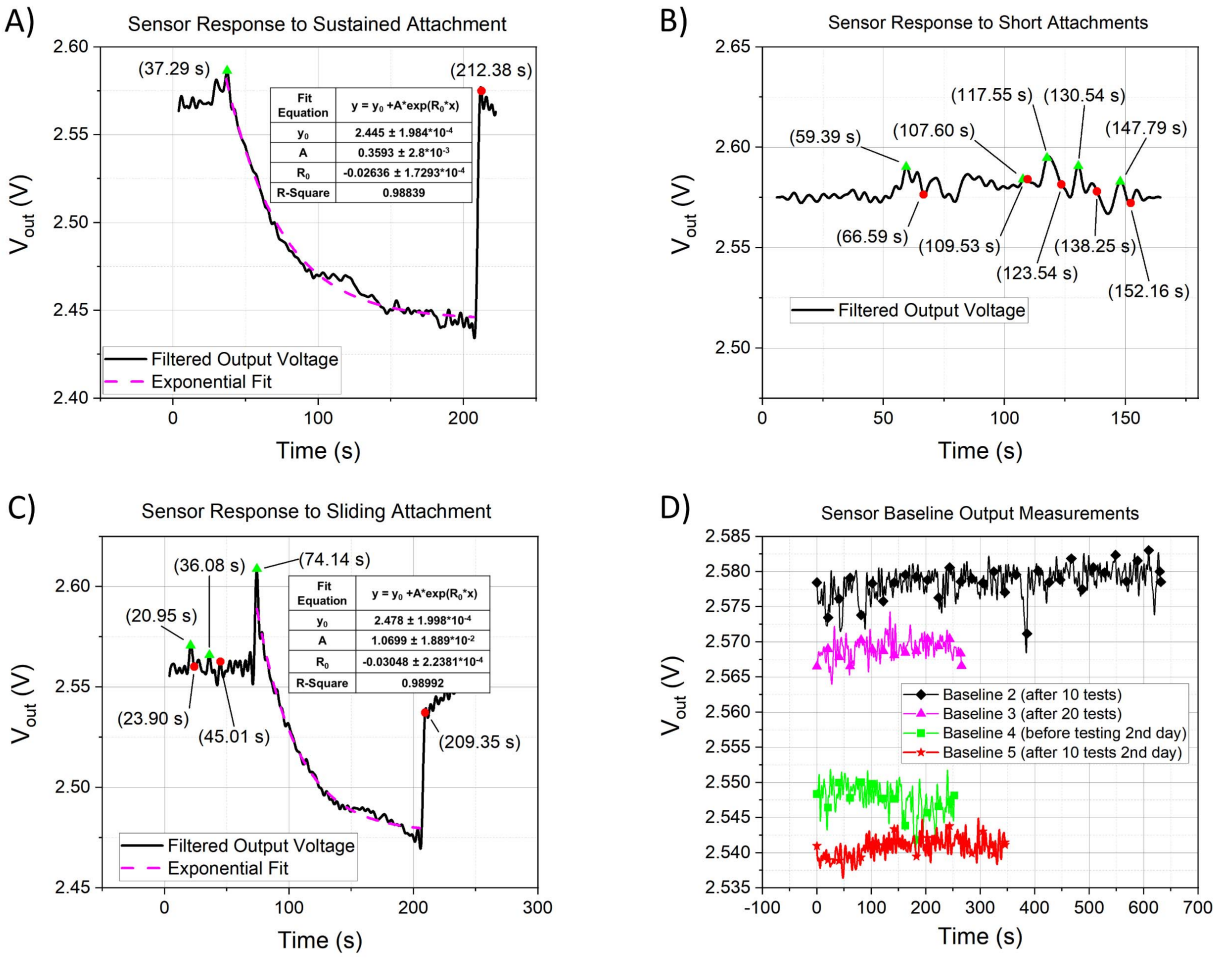

Fig. 3. (a) Sensor response to a sustained sea lamprey attachment event; (b) Sensor response to short sea lamprey attachment events; (c) Sensor response to a sliding attachment event; (d) Compilation of baseline measurements taken throughout testing.

The following discussion is focused on three tests that are representative of these responses, but Section 2 of the supplementary information of this manuscript contains the remaining experimental results. Fig. 3-A shows a representative measurement of the sensor response to a sustained lamprey attachment. It can be noticed in the video for this test (see supplementary material video S1), the lamprey's attachment to the sensor at t = 37.29 s and detachment at t = 212.38 s, denoted on the plot through colored markers with green indicating attachment to the panel and red indicating release. The output voltage of the sensor (Vout) shows a clear exponential decay to a DC value below the original baseline when the lamprey attached, corresponding to an increase in the resistance observed between the IDEs (R_{IDE}), with a sudden change back to baseline when it detaches. The observed response suggests that the system is not a purely resistive circuit. Instead, it includes reactive components that result in a time-dependent response characteristic of a first-order transient circuit, which is to be expected as water and living tissue are known dielectric materials. This behavior presents an opportunity to model this type of interaction using discrete circuit components, which will be discussed in Section 4.

The next plot shown in Fig. 3-B is representative of the sensor response to brief attachments. During this test, the lamprey was visually observed to be attaching to the sensor multiple times for period of less than 10 seconds (see video S2 in Section 1 of the supplementary material). Each of these attachment periods is highlighted on the plot using colored data markers. While there appear to be transients in the data at these instances, the magnitude of the response of the sensor is not enough to be clearly distinguished from measurement noise. This observed behavior suggests that a minimum attachment time is needed for the sensor response to be detectable, which supports the time dependency of the exponential decay response represented in Fig. 3-A.

Fig. 3-C shows the sensor response when the lamprey slid onto the sensor traces after attaching partially or completely outside of the sensing area. In the video recording of this test (video S3 in Section 1 of the supplementary material), two quick attachments directly onto the sensing area are observed, before a third attachment occurs where the lamprey only partially covers the sensor. At this point the handler slid the lamprey across the device to bring it to a central position on the panel. As seen in Fig. 3-B the quick attachments did not generate a response distinguishable from measurement noise. However, while the characteristic exponential decay of a sustained attachment seen in Fig. 3-A is still observed, it is now preceded by a large transient spike caused by the lamprey

Authorized licensed use limited to: Michigan State University. Downloaded on February 28,2022 at 16:02:46 UTC from IEEE Xplore. Restrictions apply.

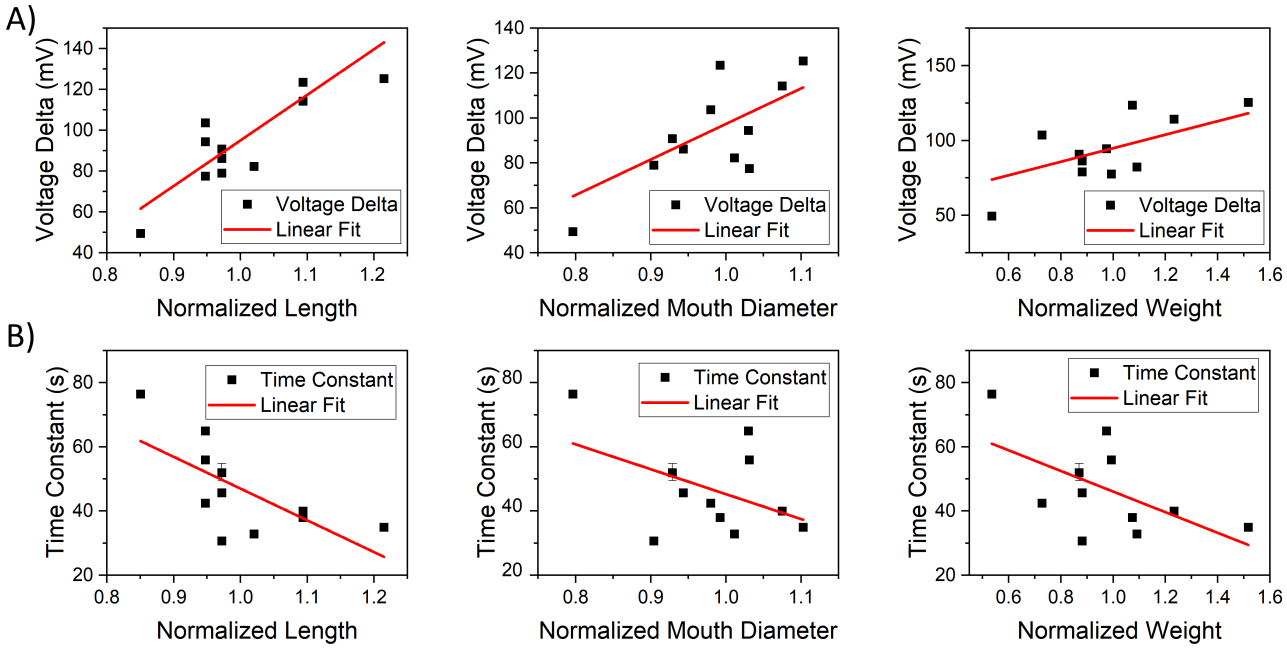

Fig. 4. (a) Correlation study between sea lamprey size parameters and voltage delta response parameter; (b) Correlation study between sea lamprey size parameters and time constant response parameter.

sliding on the sensor. This transient indicates that this attachment method somehow reduces the resistance seen across the IDE sensor for a very brief period before it begins to increase – resembling the observation for a direct, sustained lamprey attachment. The mechanism behind this phenomenon is still not fully understood; though it may be that the movement of the lamprey is contributing to a quick discharging of the double layer capacitance that naturally forms between a conductor and ionic liquid in contact when subjected to an electric field, briefly creating a current path with resistance smaller than the ionic solution's bulk resistance.

B. Response Validation

Since the responses of the sensor to the three attachment types that were identified during testing have been presented, it is also necessary to examine the baseline measurements of our device to determine its reliability and susceptibility to false positives. The plot shown in Fig. 3-D contains the results of each baseline measurement test taken throughout our experiments. For easier viewing, the individual plots are available to reader in the supplementary material's Section 3. While there exists measurement noise in the baseline, there is a clear and stable average V_{out} value for each of the tests. This value does vary slightly from test to test, indicating some drift, but these could be attributed to variances in water temperature as the water in the tanks is taken directly from Lake Huron, which experiences some slight temperature variations throughout the day. Regardless of the cause, these variations not only appear to be much smaller than the sensor response to a lamprey attachment event, but they also occur over a timescale of hours meaning they could be easily distinguished from the sensor's characteristic exponential decay response. Additionally, this stability of the measured baseline was maintained even after a total of 30 experiments across two days, thus providing strong support to the robustness of the device.

IV. Analysis

As explained in the previous section, whenever there was a sustained lamprey attachment on the developed sensor (whether by direct attachment or sliding) an exponential decay was observed at the output voltage of the sensor (V_{out}). This type of response can be characterized by the time constant of the decay along with the steady state value of the response. Considering the sea lamprey attachment time period, the response voltage can be modeled as

$$V_{out} = V_{baseline} - \Delta V \left(1 - e^{-\frac{t}{\tau}}\right) \tag{3}$$

where τ is the time constant of the decay and $V_{baseline}$-ΔV is the value of V_{out} at steady state. These parameters can be extracted from an exponential fit to the measurements where a sustained lamprey attachment was observed, and then used to explore their correlation to sea lamprey characteristics, such as length, weight, and mouth diameter. The exponential fit tool from OriginLab was used, which uses the following exponential relationship

$$y = y_0 + Ae^{R_0 x} \tag{4}$$

Seventy percent of the first day's tests presented the characteristic exponential decay corresponding to the sustained attachment and sliding attachment cases. With a few exceptions, detailed in the supplementary material Section S2, these tests were used for the correlation study. The other remaining tests showed behavior that resembled that of intermittent contact – i.e., not sustained mouth attachment – to the sensor (see Fig. 3-B). The baseline voltage ($V_{baseline}$) was obtained on a test-by-test basis, by taking the average of the response before the exponential decay occurs. The change in voltage

Authorized licensed use limited to: Michigan State University. Downloaded on February 28,2022 at 16:02:46 UTC from IEEE Xplore. Restrictions apply.

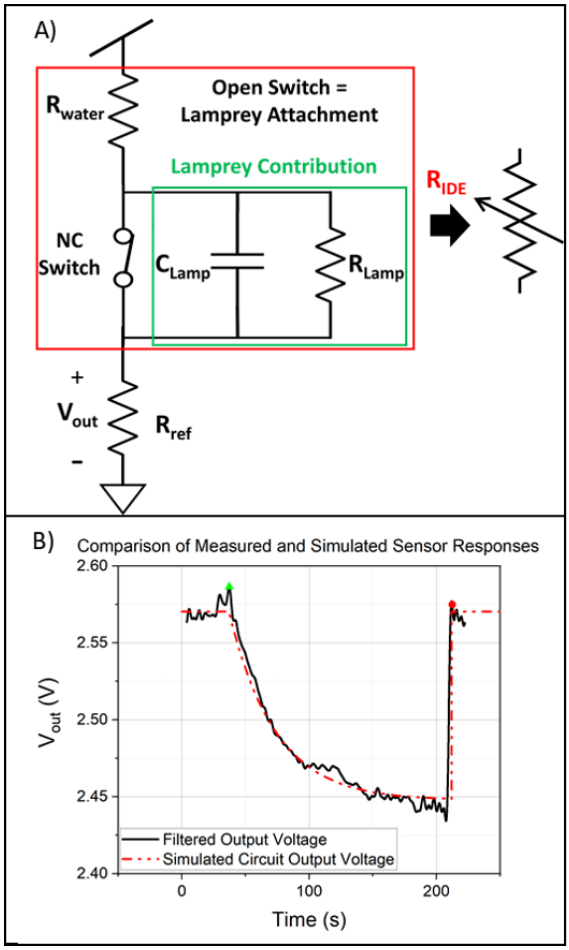

Fig. 5. (a) Schematic of representative electrical circuit; (b) Comparison on simulated circuit output with measured response.

(ΔV) was calculated by subtracting the steady state value (y_0) from the exponential fit from the baseline value. Fig. 4-A shows the result of the correlation study between ΔV and the lamprey size parameters.

In order to reduce spread on the x-axis, the size parameters are normalized with respect to the median value of each parameter of the entire 20 lamprey cohort. value of each parameter of the entire 20 lamprey cohort. The values of ΔV are plotted along with the corresponding error bars obtained from the fit. The plots shown in Fig. 4-A show a weak positive linear correlation between all size parameters and the ΔV of the measured response, indicating that larger lamprey had a larger response magnitude than smaller lampreys.

The next parameter that was studied is the time constant, which was obtained from the fit equation as $\tau = -1/R_0$ seconds. The results of the correlation study between the lamprey size parameters and τ are shown in Fig. 4-B. The plots show a weak negative correlation between the time constant and the lamprey size parameters, indicating that larger lampreys within our sample produce sensor responses with smaller time constants, implying smaller capacitance, which correspond to a faster decay to the attachment baseline. Although these are promising results toward a contact sensor that can distinguish between invasive and native lamprey species, it is important to recognize that the relatively small sample size (20 male sea lamprey) used in this study is not sufficient to establish a generalized relationship between the lamprey size parameters and the response parameters. Additionally, we are not considering if there exists any cross-correlation between the lamprey size parameters themselves. Because of the pattern observed between oral disk size and sensor response parameters, partial attachment cases where the lamprey is not completely covering the sensor, could also be problematic; in these cases, the sensor could respond as if a smaller lamprey was attached allowing for possible misclassification. However, this effect may be mitigated by using an array of these sensors, rather than a single unit. As mentioned in the results, the exponential decay suggests the lamprey-sensor interaction can be represented by an RC circuit lumped model. A finite element model (FEM) simulation of the lamprey-sensor interaction corroborating the parallel RC circuit behavior is provided in the supplementary material (Section 4). The simplest circuit that would result in the observed behavior is shown in Fig. 5-A.

In this circuit, the attachment of the lamprey is represented as a normally-closed switch (NC Switch in schematic) that opens upon lamprey attachment, forcing the series connection of a simple parallel RC circuit to the conduction path. When the switch is triggered (i.e., switch is opened), the capacitor initially behaves as a short circuit, causing the current to bypass the parallel resistor (R_{Lamp}); but after that initial transient behavior, the capacitor begins to accumulate charge and behaves more like an open circuit, thus sending more current to the parallel resistor. This has the effect of gradually introducing the resistor into the current path, which results in a wave form like the one observed during testing. The effective values of the electric lumped model shown in Fig. 5-A can be extracted from the exponential fit shown in Fig. 3-A. Since a sudden change in V_{out} is not observed at the instant the lamprey attaches, it is reasonable to assume that the baseline resistance somehow stays in the conduction path. Therefore, the steady state voltage is the result of the following voltage divider:

$$V_{out} = y_0 = \frac{V_{DC} * R_{ref}}{R_{ref} + R_{water} + R_{lamp}} \tag{5}$$

Note that the value of the resistance due to water is different from R_{ref}, as the baseline output voltage before the lamprey attaches was not exactly 2.50 V. However, R_{water} can be readily obtained by solving for R_{IDE} in (1) using the measured values of V_{out} before any lamprey activity is initiated. Once the value of R_{Lamp} is obtained, it can be used to determine the corresponding capacitance value, since $\tau = R_{lamp}C_{lamp}$.

Simulation of the proposed circuit using the values obtained from this analysis was performed using LTspice XVII and the response of the circuit is shown in Fig. 5-B, along with the experimental measurement. The simulation shows the exponential decay behavior when the switch opens (corresponding to the lamprey attachment) and a sudden return to baseline when the switch is closed (corresponding to the lamprey releasing from the panel). The simulation, however, does not capture the behavior of the sensor response to a sliding attachment, which could be viewed as a ramp input to the

Authorized licensed use limited to: Michigan State University. Downloaded on February 28,2022 at 16:02:46 UTC from IEEE Xplore. Restrictions apply.

system and would require a more complex circuit lumped model.

V. Conclusion

A simple and effective IDE sensor for lamprey attachment detection was demonstrated. Three different categories of sensor response were identified, corresponding to different attachment types: sustained, short, and sliding-sustained. Whereas the response due to short attachments was not distinguishable from measurement noise, the other two response categories showed a characteristic exponential decay shape. The measured voltage at steady state and the time constant of the response were identified as parameters that may be used to obtain information about the lamprey's physical characteristics, which could allow classification of the attached lamprey, although confirmation would require further testing with larger samples sizes. The correlation study performed between the response parameters and the lamprey size parameters showed a weak linear correlation between them. The voltage change appeared to have a positive correlation with all the lamprey size parameters studied (length, weight and mouth diameter), i.e., bigger lamprey generated a sensor response with a larger change in voltage, whereas the time constant had a negative correlation with every lamprey size parameter. Expansion of the system into an array of these devices may help mitigate possible issues that arise in the case of partial attachments, by expanding the effective sensing area without sacrificing device sensitivity. We proposed a representative circuit to model the lamprey-sensor interaction and simulated it using element values extracted from the parameters of the measured experimental response. The simulated circuit matched the behavior observed in the experimental data for the case of sustained lamprey attachment. The case of sliding-sustained attachment would require a more complex circuit lumped model that can account for a ramp-type response, which is the subject of future work.

The device presented in this work could serve as the basis for a remote sensing system to continuously monitor lamprey populations in the tributaries of the Great Lakes without the need to physically capture individual animals. Like the current trap-based assessment program, the value of such a system would invariably depend on the degree of interaction between sea lampreys and these remote sensing devices during spawning migration. Though sea lampreys are commonly observed attached to both natural and artificial substrates during the adult life stage, little is understood about the factors that influence attachment during migration, such as whether attachment rates vary by season, maturation, time of day, or substrate. Future work directed at those critical uncertainties will be needed to determine the size, number, and distribution of sensors to detect a desired number or proportion of sea lampreys in a tributary and to determine if detected lampreys are representative of each population therein. Further improvements to the system hardware will also be necessary, including additional ruggedization of the sensor, expansion into sensor arrays, waterproofing for supporting electronics, and adding data storage/transmission modules. Software enhancement of the system through the use of machine learning to improve identification of invasive sea lamprey is also possible. Additionally, flexible conductive materials could be explored to create sensors which could conform to places lampreys naturally attach to and allow for more versatile placement of these sensors throughout the tributary systems.

Acknowledgment

The authors of this paper would like to thank Trisha Searcy (USGS) for her assistance during testing. All sea lamprey experiments were performed in accordance with protocols and guidelines approved by Michigan State University's Institutional Animal Care and Use Committee (IACUC, No. 02/18-028-00). Any description of products or firm names is for descriptive purposes only and does not imply endorsement by the U.S. Government.

References

[1] C. B. Renaud and P. A. Cochran, "Post-metamorphic feeding in lampreys," in *Lampreys: Biology, Conservation and Control*, vol. 2, M. F. Docker, Ed. Dordrecht, The Netherlands: Springer, 2019, pp. 247–285.

[2] R. L. Eshenroder, "The role of the Champlain Canal and Erie Canal as putative corridors for colonization of Lake Champlain and Lake Ontario by sea lampreys," *Trans. Amer. Fisheries Soc.*, vol. 143, no. 3, pp. 634–649, May 2014, doi: 10.1080/00028487.2013.879818.

[3] V. C. Applegate. (1950). *Natural History of the Sea Lamprey, Petromyzon Marinus, in Michigan*. Report. [Online]. Available: http://pubs.er.usgs.gov/publication/70171151

[4] B. R. Smith and J. J. Tibbles, "Sea lamprey *(Petromyzon marinus)* in Lakes Huron, Michigan, and Superior: History of invasion and control, 1936–78," *Can. J. Fisheries Aquatic Sci.*, vol. 37, no. 11, pp. 1780–1801, Nov. 1980. [Online]. Available: https://cdnsciencepub-com.proxy2.cl.msu.edu/doi/abs/10.1139/f80-222

[5] W. J. Christie, "Changes in the fish species composition of the great lakes," *J. Fisheries Res. Board Canada*, vol. 31, no. 5, pp. 827–854, May 1974, doi: 10.1139/f74-104.

[6] A. Muir, C. Krueger, and M. Hansen, "Re-establishing lake trout in the Laurentian Great Lakes: Past, present, and future," in *Great Lakes Fisheries Policy and Management: A Binational Perspective*. East Lansing, MI, USA: Michigan State Univ. Press, 2013, pp. 533–588.

[7] W. J. Christie, "Changes in the fish species composition of the Great Lakes," *J. Fisheries Board Canada*, vol. 31, no. 5, pp. 827–854, 1974.

[8] J. E. Marsden and M. J. Siefkes, "Control of invasive sea lamprey in the Great Lakes, Lake Champlain, and Finger Lakes of New York," in *Lampreys: Biology, Conservation and Control*, vol. 2, M. F. Docker, Ed. Dordrecht, The Netherlands: Springer, 2019, pp. 411–479.

[9] *Great Lakes Fishery Commission—The Fishery*. Accessed: Mar. 4, 2021. [Online]. Available: http://www.glfc.org/the-fishery.php

[10] R. A. Bergstedt, R. B. McDonald, K. M. Mullett, G. M. Wright, W. D. Swink, and K. P. Burnham, "Mark-recapture population estimates of parasitic sea lampreys *(Petromyzon marinus)* in Lake Huron," *J. Great Lakes Res.*, vol. 29, pp. 226–239, Jan. 2003, doi: 10.1016/S0380-1330(03)70491-2.

[11] M. J. Hansen, C. P. Madenjian, J. W. Slade, T. B. Steeves, P. R. Almeida, and B. R. Quintella, "Population ecology of the sea lamprey *(Petromyzon marinus)* as an invasive species in the Laurentian great lakes and an imperiled species in Europe," *Rev. Fish Biol. Fisheries*, vol. 26, no. 3, pp. 509–535, Sep. 2016, doi: 10.1007/s11160-016-9440-3.

[12] T. D. Gingera, T. B. Steeves, D. A. Boguski, S. Whyard, W. Li, and M. F. Docker, "Detection and identification of lampreys in great lakes streams using environmental DNA," *J. Great Lakes Res.*, vol. 42, no. 3, pp. 649–659, Jun. 2016, doi: 10.1016/j.jglr.2016.02.017.

[13] H. Shi *et al.*, "Screen-printed soft capacitive sensors for spatial mapping of both positive and negative pressures," *Adv. Funct. Mater.*, vol. 29, no. 23, Jun. 2019, Art. no. 1809116, doi: 10.1002/adfm.201809116.

[14] X. Tan. (Jan. 14, 2020). *E-Skin Technology Could Aid in Sea Lamprey Fight*. Accessed: May 2021. Great Lakes Connection Newsletter, International Joint Commission. [Online]. Available: https://ijc.org/en/e-skin-technology-could-aid-sea-lamprey-fight

Authorized licensed use limited to: Michigan State University. Downloaded on February 28,2022 at 16:02:46 UTC from IEEE Xplore. Restrictions apply.

[15] R. D. Adams, "Suction pressure measurement and behavioral observations of spawning-run sea lampreys (Petromyzon marinus)," M.S. thesis, Biol. Dept. Eastern Michigan Univ, Ypsilanti MI, USA, 2006.
[16] H. Shi, C. M. Holbrook, Y. Cao, N. Sepúlveda, and X. Tan, "Measurement of suction pressure dynamics of sea lampreys, *Petromyzon marinus*," *PLoS ONE*, vol. 16, no. 4, Apr. 2021, Art. no. e0247884, doi: 10.1371/journal.pone.0247884.
[17] J. G. Guan, Q. YU Miao, and Q. J. Zhang, "Impedimetric biosensors," *J. Biosci. Bioeng.*, vol. 97, no. 4, pp. 219–226, 2004.
[18] N. Hikmah, H. F. Hawari, and M. Gupta, "Design and simulation of interdigitated electrode for graphene-SnO_2 sensor on acetone gas," *Indonesian J. Electr. Eng. Comput. Sci.*, vol. 19, no. 1, p. 119, Jul. 2020, doi: 10.11591/ijeecs.v19.i1.pp119-125.
[19] L. Wang, M. Veselinovic, L. Yang, B. J. Geiss, D. S. Dandy, and T. Chen, "A sensitive DNA capacitive biosensor using interdigitated electrodes," *Biosens. Bioelectron.*, vol. 87, pp. 646–653, Jan. 2017, doi: 10.1016/j.bios.2016.09.006.
[20] J. Wang, C. Wu, N. Hu, J. Zhou, L. Du, and P. Wang, "Microfabricated electrochemical cell-based biosensors for analysis of living cells in vitro," *Biosensors*, vol. 2, no. 2, pp. 127–170, Apr. 2012, doi: 10.3390/bios2020127.
[21] P. Van Gerwen *et al.*, "Nanoscaled interdigitated electrode arrays for biochemical sensors," *Sens. Actuators B, Chem.*, vol. 49, no. 1, pp. 73–80, 1998, doi: 10.1016/S0925-4005(98)00128-2.
[22] J. S. Daniels and N. Pourmand, "Label-free impedance biosensors: Opportunities and challenges," *Electroanalysis*, vol. 19, no. 12, pp. 1239–1257, Jun. 2007, doi: 10.1002/elan.200603855.
[23] C. Gaul. (2019). *Lampetra Appendix*. (On-Line), Animal Diversity Web. Accessed: Jul. 28, 2021. [Online]. Available: https://animaldiversity.org/accounts/Lampetra_appendix/
[24] B. Karvel-Fuller. (2013). *Ichthyomyzon Fossor*. (On-Line), Animal Diversity Web. Accessed: Jul. 28, 2021. [Online]. Available: https://animaldiversity.org/accounts/Ichthyomyzon_fossor/
[25] T. Acciaioli. (2014). *Ichthyomyzon Castaneus*. (On-Line), Animal Diversity Web. Accessed: Jul. 28, 2021. [Online]. Available: https://animaldiversity.org/accounts/Ichthyomyzon_castaneus/
[26] C. Blumbergs. (2014). *Ichthyomyzon Unicuspis*. (On-Line), Animal Diversity Web. Accessed: Jul. 28, 2021. [Online]. Available: https://animaldiversity.org/accounts/Ichthyomyzon_unicuspis/
[27] A. Dizon and M. E. Orazem, "On the impedance response of interdigitated electrodes," *Electrochimica Acta*, vol. 327, Dec. 2019, Art. no. 135000, doi: 10.1016/j.electacta.2019.135000.
[28] S. Cherry. (2011). *Petromyzon Marinus*. (On-line), Animal Diversity Web. Accessed: Jul. 28, 2021. [Online]. Available: https://animaldiversity.org/accounts/Petromyzon_marinus/

Ian González-Afanador (Member, IEEE) received the B.S. degree in electrical and computer engineering from the University of Puerto Rico, Mayagüez, Puerto Rico, in 2019. He is currently pursuing the Ph.D. degree in electrical and computer engineering with Michigan State University.

He has had internships with Honeywell Aerospace and Lockheed-Martin Sikorsky and has participated in summer research programs at the University of Virginia, Michigan State University, and Georgia Tech. His current research interests include the development of underwater biological contact/accumulation and development of piezoelectric-based anti-fouling systems for light sources used in algal cultivation.

Mr. Gonzalez-Afanador was a recipient of the NSF Graduate Research Fellowship and the MSU University Distinguished Fellowship.

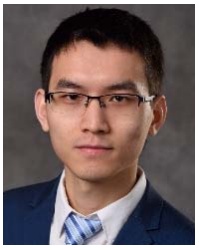

Hongyang Shi (Member, IEEE) received the B.S. degree in mechanical design, manufacturing and automation and the M.S. degree in mechatronic engineering from the Huazhong University of Science and Technology (HUST), Wuhan, China, in 2012 and 2015, respectively. He is currently pursuing the Ph.D. degree in electrical and computer engineering with Michigan State University, East Lansing, MI, USA. His research interest includes soft robotics and smart materials.

Christopher Holbrook received the Bachelor of Science and Master of Science degrees in zoology from the University of Maine, USA, and the Doctor of Philosophy degree in fisheries and wildlife from Michigan State University, USA. His research interests include fish ecology and fisheries management.

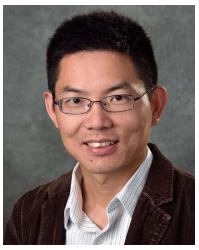

Xiaobo Tan (Fellow, IEEE) received the B.Eng. and M.Eng. degrees in automatic control from Tsinghua University, Beijing, China, in 1995 and 1998, respectively, and the Ph.D. degree in electrical and computer engineering from the University of Maryland, College Park, MD, USA, in 2002.

He is currently an MSU Foundation Professor and the Richard M. Hong Endowed Chair in Electrical and Computer Engineering at Michigan State University (MSU). His research interests include modeling and control of systems with hysteresis, electroactive polymer sensors and actuators, soft robotics, and bio-inspired underwater robots and their application to environmental sensing. He has published over 300 articles and been awarded four U.S. patents in these areas. He is a Fellow of ASME. He was a recipient of NSF CAREER Award in 2006, MSU Teacher-Scholar Award in 2010, MSU College of Engineering Withrow Distinguished Scholar Award in 2018, Distinguished Alumni Award from the Department of Electrical and Computer Engineering, University of Maryland, in 2018, and multiple best paper awards. He also serves as a Senior Editor for IEEE/ASME TRANSACTIONS ON MECHATRONICS.

Nelson Sepúlveda (Senior Member, IEEE) received the B.S. degree in electrical and computer engineering from the University of Puerto Rico, Mayagüez, Puerto Rico, in 2001, and the M.S. and Ph.D. degrees in electrical and computer engineering from Michigan State University (MSU), East Lansing, MI, USA, in 2002 and 2005, respectively. During the last year of graduate school, he attended Sandia National Laboratories. He joined the Department of Electrical and Computer Engineering, University of Puerto Rico, as a Faculty Member, in 2006. He was a Visiting Faculty Researcher at Air Force Research Laboratories in 2006, 2007, 2013, and 2014, the National Nanotechnology Infrastructure Network in 2008, and the Cornell Center for Materials Research in 2009; the last two being the National Science Foundation (NSF) funded centers at Cornell University, Ithaca, NY, USA. In 2011, he joined as a Faculty Member the Department of Electrical and Computer Engineering, MSU, where he is currently a Professor. His current research interests include smart materials and the integration of such in microelectromechanical systems, with particular emphasis on vanadium dioxide thin films and the use of the structural phase transition for the development of smart microactuators. He received the NSF CAREER Award in 2010 and the MSU Teacher Scholar Award in 2015.

Authorized licensed use limited to: Michigan State University. Downloaded on February 28,2022 at 16:02:46 UTC from IEEE Xplore. Restrictions apply.